 doi:10.20944/preprints201906.0043.v1

Hydrodynamic light flashing in thin layer wavy photobioreactors

Moroni M.[1], Lorino S.[2], Cicci A.[3], Bravi M.[2,*]

[1]Sapienza Università di Roma, Department of Civil and Environmental Engineering, Via Eudossiana 18, 00184 Rome, Italy

[2]Sapienza Università di Roma, Department of Chemical Engineering, Via Eudossiana 18, 00184 Rome, Italy

[3]Bio-P s.r.l., via di Vannina 88, 00156 Rome, Italy

*Corresponding author email: marco.bravi@uniroma1.it. postal address: via Eudossiana 18, 00184 Rome (IT).

Phone number:+390644585587

Abstract

In a thin-volume photobioreactor where a concentrated suspension of microalgae is circulated throughout the established spatial irradiance gradient, microalgal cells experience a time-variable irradiance. Deploying this feature is the most convenient way of obtaining the so-called “flashing light” effect, improving biomass production in high irradiance.

This work investigates the light flashing features of sloping wavy photobioreactors, a recently proposed type, by introducing and validating a Computational Fluid Dynamics model. Two characteristic flow zones (straight top-bottom stream and local recirculation stream), both effective toward light flashing, have been found and characterised: a recirculation-induced frequency of 3.7 Hz and straight flow-induced frequency of 5.6 Hz were estimated. If the channel slope is increased, the recirculation area becomes less stable while the recirculation frequency is nearly constant with flow rate. The validated CFD model is a mighty tool that could be reliably used to further increase the flashing frequency by optimising the design, the dimensions, the installation and the operational parameters of the sloping wavy photobioreactor.

 doi:10.20944/preprints201906.0043.v1

Keywords: microalgae; photobioreactor; flashing light effect; Computational Fluid Dynamics.

1 Introduction

Microalgae are considered as one of the most promising fast-growing photosynthetic microorganisms on Earth, hence it is expected that they can play an important role in CO2 sequestration, food, feed, sourcing of biochemical products, commodities, biofuels and for phytodepuration.

Due to the significant light attenuation along the light path [1], concentrated microalgal suspensions needs to be cultured at a little thickness to avoid reducing the volume-based specific growth rate [2], so that cells that circulate back and forth along the established spatially-distributed irradiance gradient experience a time-varying irradiance, that is a flashing light effect. The “flashing light” effect is extremely beneficial in outdoor cultures because microalgae reach their maximum photosynthetic activity at roughly 1/10 of the maximum irradiation recorded in summer days and the photosynthetic machinery is damaged by photooxidation and photoinhibition well below the maximum sunlight irradiance values [3] if light is not alternated with darkness at a proper rate. Indeed, the combination between excessive dark volume and excessive light is the main cause that limits the productivity of established commercial photobioreactors (PBRs) to one order of magnitude below the theoretical limit. The problem of light saturation and attenuation could be greatly reduced if proper combinations between cell density and mixing could be achieved, owing to the higher photosynthetic efficiency recorded when light energy exceeding the saturation intensity is supplied in short pulses rather than in a continuous flow.

Apparently, there is quite substantial discrepancy among the quantitative estimates of the benefits of light flashing, and this is at least partly due to differences in the experimental set up or assumptions concerning the operational mode of the equipment used to carry out the experimental investigation, such as the irradiance spectrum, the operational dark volume fraction of the photobioreactor, and the

Preprints (www.preprints.org) | NOT PEER-REVIEWED | Posted: 5 June 2019 doi:10.20944/preprints201906.0043.v1

culturing mode. As an example of the different conclusions that may be drawn from the recent literature it was observed that photosynthetic rates increase exponentially with increasing L/D frequency, and also depend upon: 1. the frequency of the L/D fluctuations; 2. the L/D ratio; 3. the light acclimation state of the culture (low or high irradiance); 4. the light intensity exposition history [4]. However, L/D cycles of 1 and 10 Hz were found result in a 10% lower biomass yield than in continuous light (therefore, a growth depression), while L/D cycles of 100 Hz resulted in 35% boost of biomass productivity [5]. Low-frequency, hydrodynamically-induced light pulsation was found to increase productivity by 38%-48% (depending on the cultured species) in an airlift photobioreactor featuring spatial alternation of irradiation rates creating a light pulse frequency of 10 Hz [6]. On the other hand, a significant penalty occurring when light-dark alternation in the range ~0.1 to ~0.01 Hz occurs under short lighting duty cycles and during purely autotrophic growth [7]. An important point that motivates the intricacy in the analysis of flashing light experimental data, and the consequent assessment of the growth promotion claim, resides in the difference between the specific observed growth rate of a cell population exposed to a spatially-uniform, time-varying irradiance, and that of a cell population of such density to completely absorb the impinging irradiance over the culture thickness. Complete absorption, indeed, maximises light utilisation by the culture and thus maximises areal productivity [8-9]. Mass transfer efficiency in mass-transfer limited cultures is synergic with photosynthetic activity promotion; since concentrated cultures may be mass transfer limited, care must be exerted both in designing experiment aimed at quantifying the effects of light flashing of hydrodynamic origin and in the subsequent data analysis [10]. Finally, it has been underlined that light/dark cycles with a well-defined frequency result enhancing productivity more than chaotic light/dark alternation [11].

The ways to induce fast alternation of illumination and darkness perceived by the microalgal cells beyond the slow (day/night) cycle which microalgae are normally exposed to, include: i) flashing

Preprints (www.preprints.org) | NOT PEER-REVIEWED | Posted: 5 June 2019 doi:10.20944/preprints201906.0043.v1

artificial illumination [12] and ii) hydrodynamic displacement of cells entrained in the medium experiencing differently lit zones, while the photobioreactor exposed surface is subjected to a stationary radiative field [13] In this latter case the perceived flashing is the result of the combined effect of the photobioreactor geometry, of the adopted circulation flow and of the microalgal culture characteristics (viscosity and optical density). In case of mixing-induced L/D cycles, it has been noted that algal productivity increases as the Reynolds number is increased [14]. However, high recirculation rates may depress productivity and the operation of the photobioreactor may require an excessive energy input [15]. Increased turbulence also enhances the exchange rates of nutrients and metabolites between the cells and their growth medium [16]. To achieve a hydrodynamically-induced flashing, Torzillo and others developed a novel photobioreactor design featuring a sloping, wavy-bottomed surface [17], which differs from the uniform thin layer cascade system designed by Setlik and others [18] in that it features a wavy bottom instead of a flat one. When installed with a low inclination angle, this photobioreactor features a spatial alternation of deep (wave troughs) and shallow (wave ridges) zones. Compared to many conventional culture systems this photobioreactor design: 1. features an optically thin culture that is amenable to high cell concentration which is amongst the top requirements for lowering biomass harvest costs [17]; 2. provides an efficient gas-liquid mass transfer, with a positive dependence upon specific flow rate [16] 3. features a low equipment cost (can be produced from low cost semi-finished materials); 4. has hydrodynamic features leading to regular, specific flow rate-dependent light-dark alternation which might result in increased photosynthetic activity with respect to other frequently adopted (e.g., tubular and bubble column) photobioreactor geometries [19]. It was shown that in a 15-cavity wavy-bottomed lower surface photobioreactor a local recirculation zone establishes in each cavity only at low inclinations ($\leq 6°$) and that its location changes according to the inclination slope from the lower (0° and 3°) to the upper part of each cavity (6°) [19]. Sforza and others' warning that the combination between species, external irradiance and hydrodynamic mixing

Preprints (www.preprints.org) | NOT PEER-REVIEWED | Posted: 5 June 2019 doi:10.20944/preprints201906.0043.v1

frequency must be carefully checked before investing on a specific photobioreactor installation [20] and the consideration of how burdensome experimentally investigating fluid dynamics is [19], motivate the development and validation of a computational fluid dynamics (CFD) model to foster further development of the sloping wavy-bottom photobioreactor, as shown by other authors for other novel photobioreactors [21-23]. The development of such CFD model is the object of the present work and, indeed, it provides at one time: an accurate description of hydrodynamics and an accurate estimate of the light-dark frequency experienced by microalgal cells during their travel across differently lit zones driven by neutral buoyancy.

2 Materials and method

2.1 CFD modeling of the photobioreactor

Using the CFD approach the dynamic behaviour of fluids in complex physical problems can be simulated through the numerical implementation of mathematical models. Here, the commercial software ANSYS FLUENT® was used. The numerical modelling of fluid dynamics problems involves the solution of the Navier-Stokes equations which are the mathematical formulation of mass and momentum conservation. Beyond the Navier-Stokes equation, additional transport equations are solved to represent the effect of turbulence.

Since both viscosity and density of the algal culture flowing within the photobioreactor are very similar to the viscosity and density of water (in the limit of a dilute microalgal suspension) and viscosity dependence upon suspension concentration is very limited up to a concentration of 10 g/L (Adesanya et al. 2012), the CFD models was designed for an air-water system. The VOF (Volume of Fluid) method was chosen to track the interface between microalgal suspension phase and the upper gas phase [24]. This approach introduces the volume fraction α_q, defined as the fraction of the cell's volume occupied

Preprints (www.preprints.org) | NOT PEER-REVIEWED | Posted: 5 June 2019 doi:10.20944/preprints201906.0043.v1

by the phase q. Said volume fractions were solved to track the interface of the air-water system (continuity equation for the volume fraction of the water phase) and to calculate the values of the needed fluid properties (density and viscosity).

The fluid flowing through the photobioreactor was simulated for two different slopes (6° for model setup and validation and 9° for model application). Considering the channel geometry and the feeding condition, the flow is mainly two-dimensional; therefore, 2D models were used to save computational time.

The model of the wavy-bottomed channel photobioreactor at slope 6° is shown in Figure 1; the model of the channel inclined at 9° is identical to the 6° one in every aspect but the inclination slope. To limit the computational burden, a 5-cavity channel was implemented instead of a 15-cavity model mimicking the experimental channel. Tests were carried out to verify that a fully developed flow was attained in each modelled cavity and that the CFD model was, therefore, equivalent to the 15-cavity channel used in the experiments (test results shown in the Supplementary material).

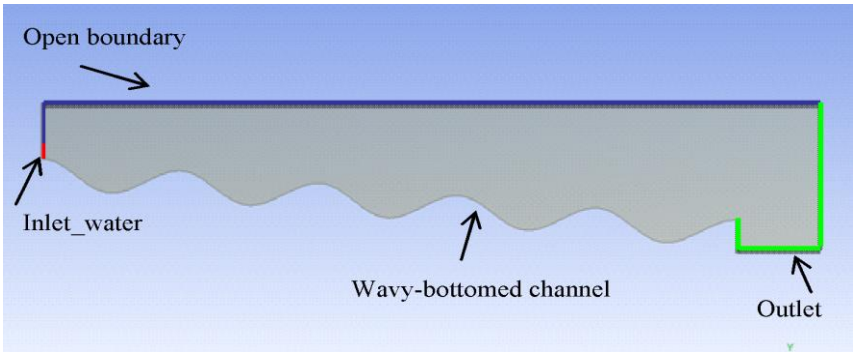

Figure 1. The model geometry and boundary conditions of the photobioreactor at slope 6°.

Boundary conditions are required on all the boundaries of the solution domain to define a specific fluid flow. In the present work, water is injected in the domain through a 0.015 m high aperture specifying its mass flow; referring to a 1 m wide channel, three flow rates per unit width were investigated,

Preprints (www.preprints.org) | NOT PEER-REVIEWED | Posted: 5 June 2019 doi:10.20944/preprints201906.0043.v1

$q_1=1.11\times10^{-3}$ m^3 s^{-1} m^{-1}, $q_2=1.48\times10^{-3}$ m^3 s^{-1} m^{-1} and $q_3=1.85\times10^{-3}$ m^3 s^{-1} m^{-1}, respectively. No remarkable influence water inlet height on the results was noticed.

Atmospheric pressure was specified at the outlet, at the boundary above the inlet and at the top boundary. Lastly, the wavy-bottom channel was modelled as a no-slip wall boundary (Figure 1).

A second-order discretization scheme was chosen for the momentum, turbulent kinetic energy and the specific dissipation rate equations; the body force-weighted pressure discretization scheme was used because of the presence of gravity, and the "Geometric Reconstruction" method was successful in sharpening the interface between air and water. The k-ω turbulent Shear Stress Transport (SST) model was adopted to solve the closure scheme owing to the low Reynolds number (in the transitional zone) characterizing the flow under investigation. The PISO algorithm was employed as the solver because it is specifically designed for transient simulations and a time step of 10^{-4} s was used to keep the simulation stable. The type, quadrangular vs. triangular cells, and size of the calculation grid was chosen based on a trade-off between accuracy in describing the interface and the computational time issue. Each simulation was extended until a stable velocity field was obtained, wherefrom the recirculation time in each cavity and the time required for a neutrally buoyant particle to travel from one cavity to the subsequent one, thus determining the light flashing experienced by cells in an operating photobioreactor of this type, can be calculated. How the steady-state condition was reached and the influence of the gridding scheme on the velocity profile are aspects fully documented in the Supplementary Material.

2.2 Experimental investigation

Model setup was based on experimental data collected in a test rig substantially analogous to that described by Moroni and others [19]. The wavy-bottomed channel, comprising 15 complete cavities (Figure 2), was installed at 6° slope and operated at the flow rates of $Q_1=0.6$ m^3/h, $Q_2=0.8$ m^3/h and

Preprints (www.preprints.org) | NOT PEER-REVIEWED | Posted: 5 June 2019 doi:10.20944/preprints201906.0043.v1

Q_3=1.0 m^3/h, corresponding to the specific flow rates numerically investigated. The Reynolds number (Re=(Q/W)/ν where Q is the flow rate, W=0.15 m is the channel width, ν is the kinematic viscosity of water) increases with flow rate, ranging between 1110 and 1850. Re values suggest that the flow regime within the channel is in the transitional regime.

The experimental investigation was carried out by feeding the channel with mixtures of water and a neutrally-buoyant tracer via a variable height tank connected to the diffuser installed at the upper-most cavity of the channel and taking a high-speed video of the flow. The image sequences were elaborated by the Hybrid Lagrangian Particle Tracking [25] (HLPT) to obtain the trajectories and the velocity fields of the tracer particles. The HLPT algorithm is based on the solution of the optical flow equation and selects areas of each image where strong brilliance gradients exist. Such areas can be associated to tracer particles and are good features to track from frame to frame. Once the particles have been identified, the algorithm calculates the coordinates of the barycenter and reconstructs the trajectory of each particle, calculating their displacement in the subsequent frames.

Image processing was achieved in three steps: 1) a pre-processing step aimed to remove the background and improve image contrast; 2) particle detection and temporal tracking via HLPT to isolate particles and track them in consecutive frames; 3) post-processing to obtain the relevant flow parameters [19].

The free surface, which from a finite distance appears as a thick zone due to the divergence of the optical axes, was excluded from the analysis.

Preprints (www.preprints.org) | NOT PEER-REVIEWED | Posted: 5 June 2019 doi:10.20944/preprints201906.0043.v1

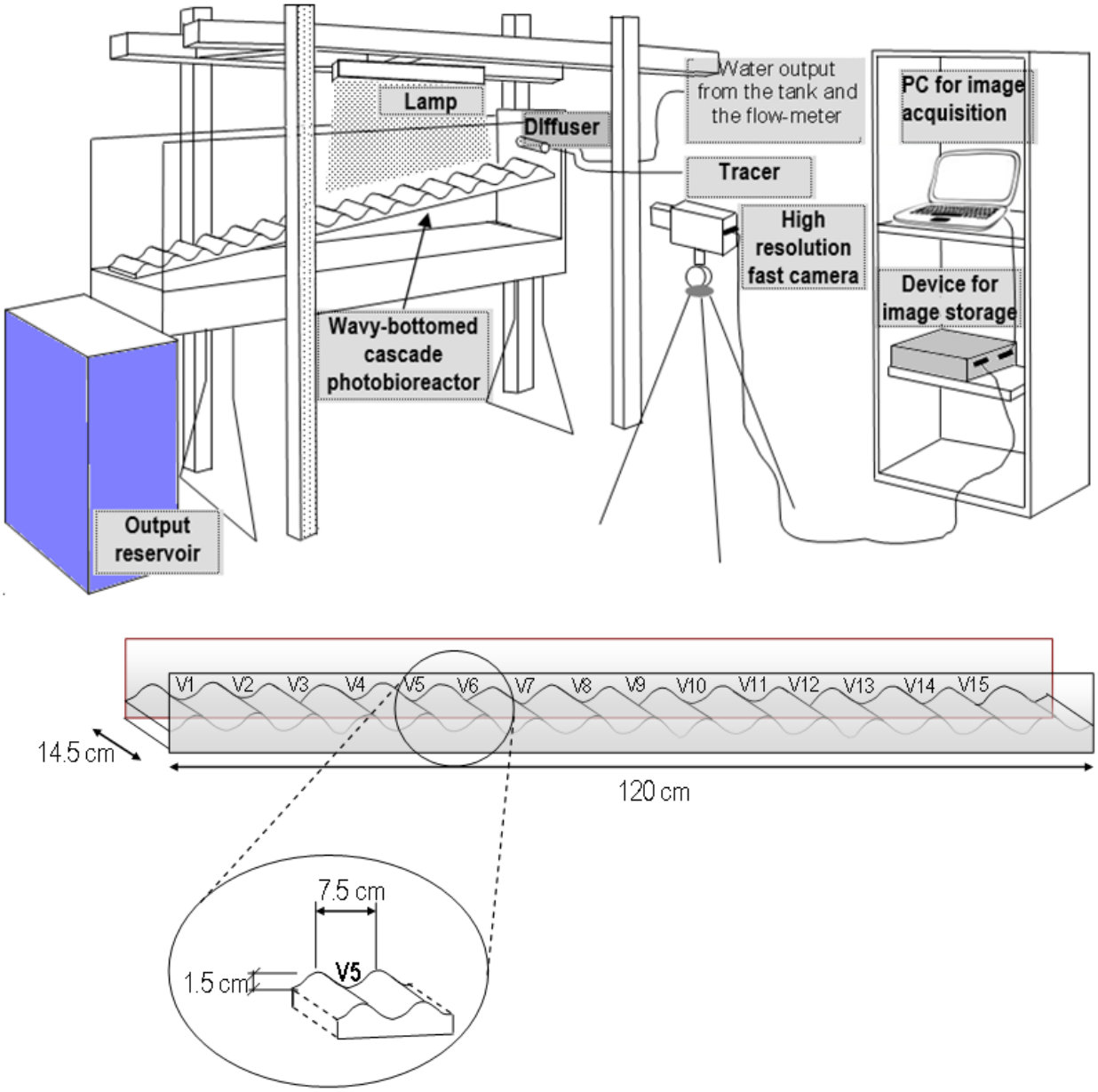

Figure 2. Experimental set-up and channel feature characteristic dimensions. V stands for vane.

3 Results

The model prediction of the velocity field and streamlines is shown in Figure 3 (the complete set of predictions can be found in the Supplementary Materials file). It shows a transport stream flowing on the bottom of the channel and a recirculation zone which steadily occupies the central part of the cavities and represent fairly well the hydrodynamic features obtained from the experimental investigation (Figure 4).

Preprints (www.preprints.org) | NOT PEER-REVIEWED | Posted: 5 June 2019 doi:10.20944/preprints201906.0043.v1

Semi-quantitative validation of the numerical model based on visually judging the agreement of the velocity profiles along the vertical section passing through the vortex center for the three experimentally tested and computationally simulated flow rates shows quite a good agreement for the minimum and the intermediate flow rate, with a substantial adherence both in the trend and in the local values of velocity (Figure 5a and Figure 5b). In the case of the maximum flow rate, the adherence between predicted and measured values of local velocity appears remarkable up to the height at which experiments allow estimating the local velocity vectors (Figure 5c).

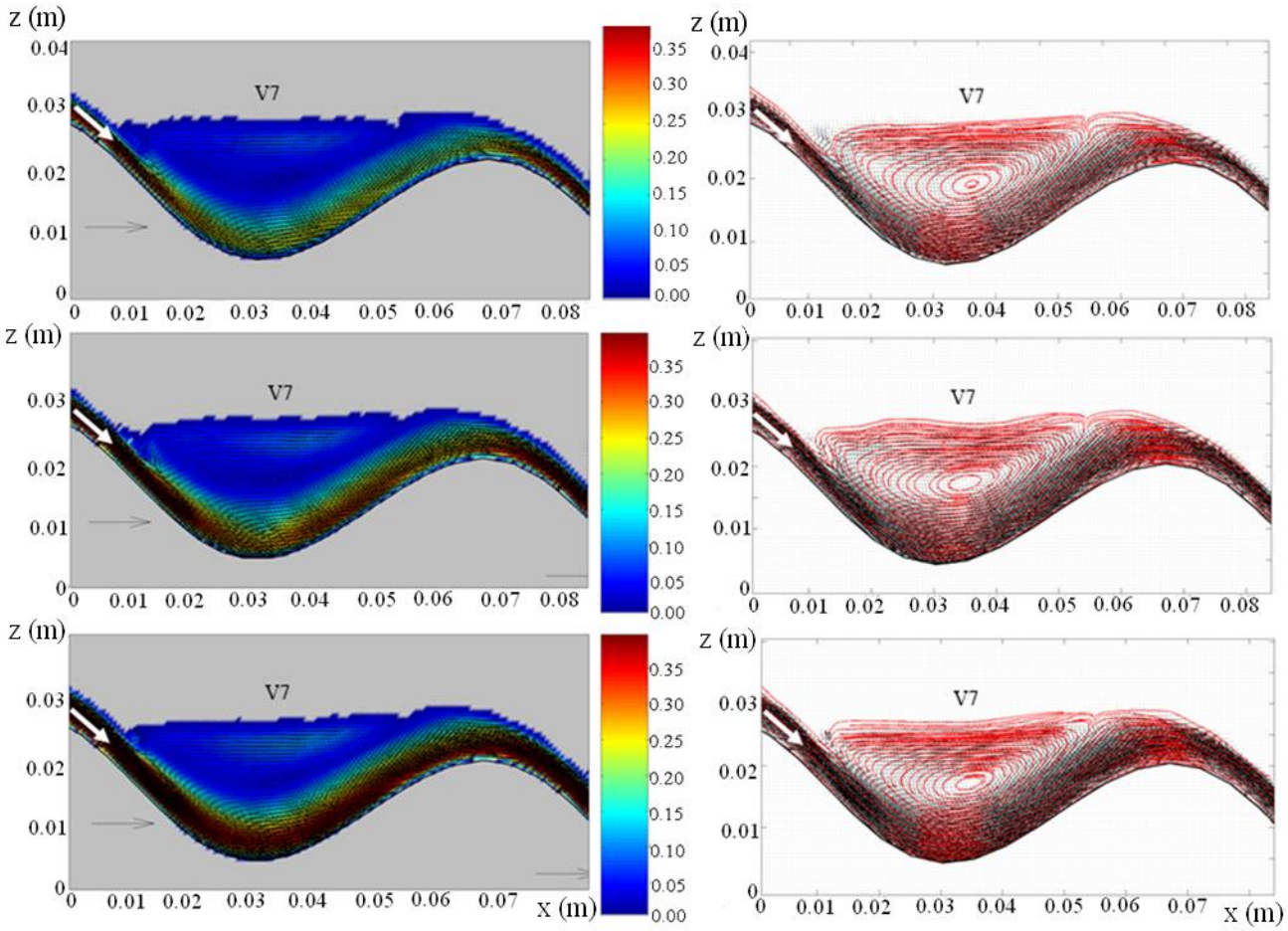

Figure 3. CFD results colormaps for 6° slope and flow rate per unit width a) q_1; b) q_2 and c) q_3; Streamlines at flow rate per unit width d) q_1; e) q_2 and f) q_3

A quantitative validation of the numerical model was performed by comparing the corresponding numeric values of the parameters describing the hydraulic features of potential photobiological

Preprints (www.preprints.org) | NOT PEER-REVIEWED | Posted: 5 June 2019 doi:10.20944/preprints201906.0043.v1

significance, and of most concern for microalgal technology. The recirculation period (t_c) of the liquid elements were calculated as $t_c = 2\pi/(\partial u/\partial z)$ from the velocity plot, by considering the (nearly) constant value of the velocity gradient within the vortex ($\partial u/\partial z$) and the characteristic dimension of the vorticose structure according to a previously described procedure [19].

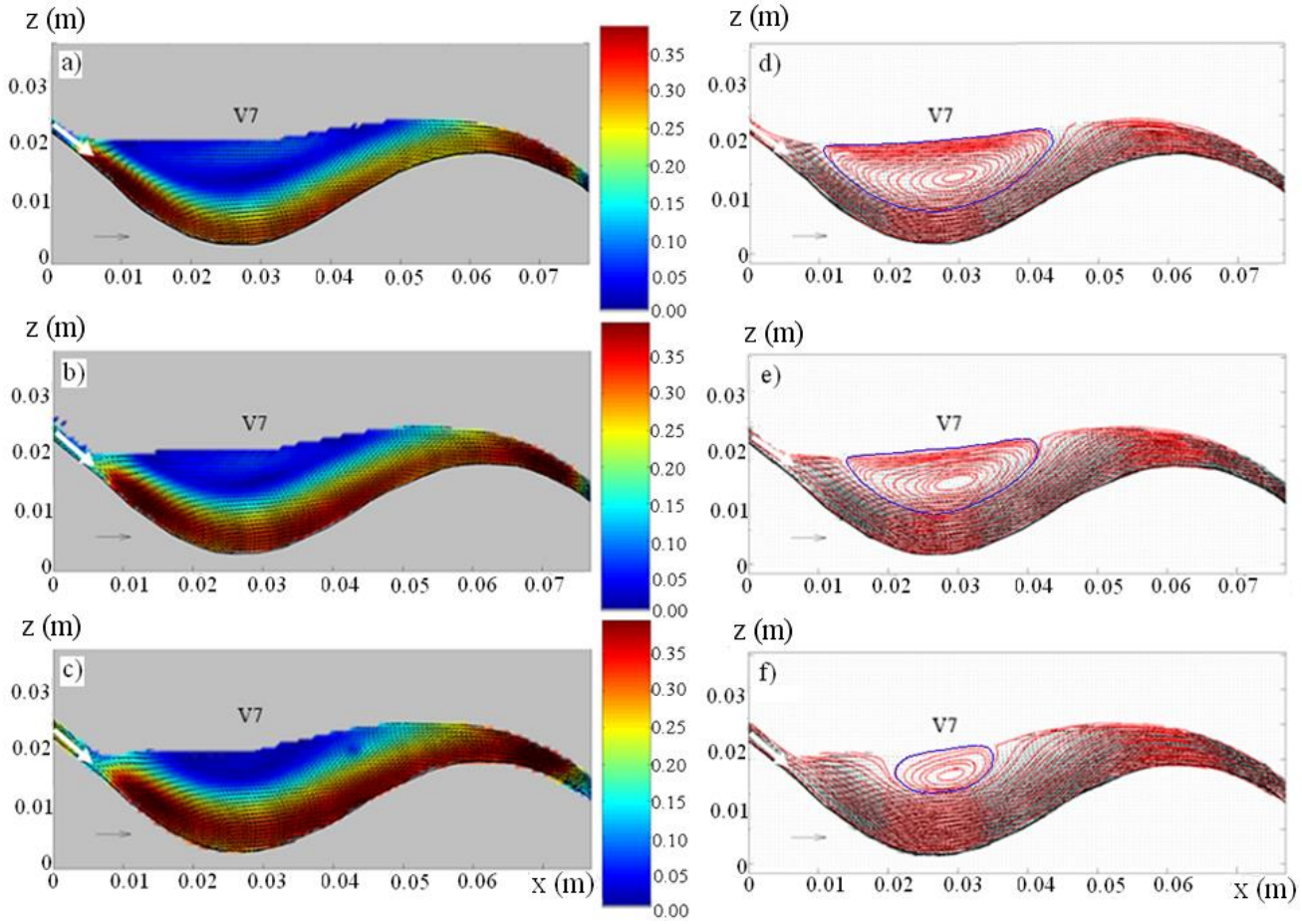

Figure 4. Experimental results colormaps for 6° slope and flow rate per unit width a) q_1; b) q_2 and c) q_3; Streamlines at flow rate per unit width d) q_1; e) q_2 and f) q_3

For the numerical simulations, the transport stream flow transit time was calculated by averaging the time required for individual "virtual tracers" (a feature of the Fluent environment) to travel the distance between two subsequent ridges of the wavy bottom. The size of the recirculation zone and the ratio

Preprints (www.preprints.org) | NOT PEER-REVIEWED | Posted: 5 June 2019 doi:10.20944/preprints201906.0043.v1

among the cross-section of fluid entrained in the thumbling structure and the entire fluid cross-section occupying each cavity, was calculated from the streamlines plots.

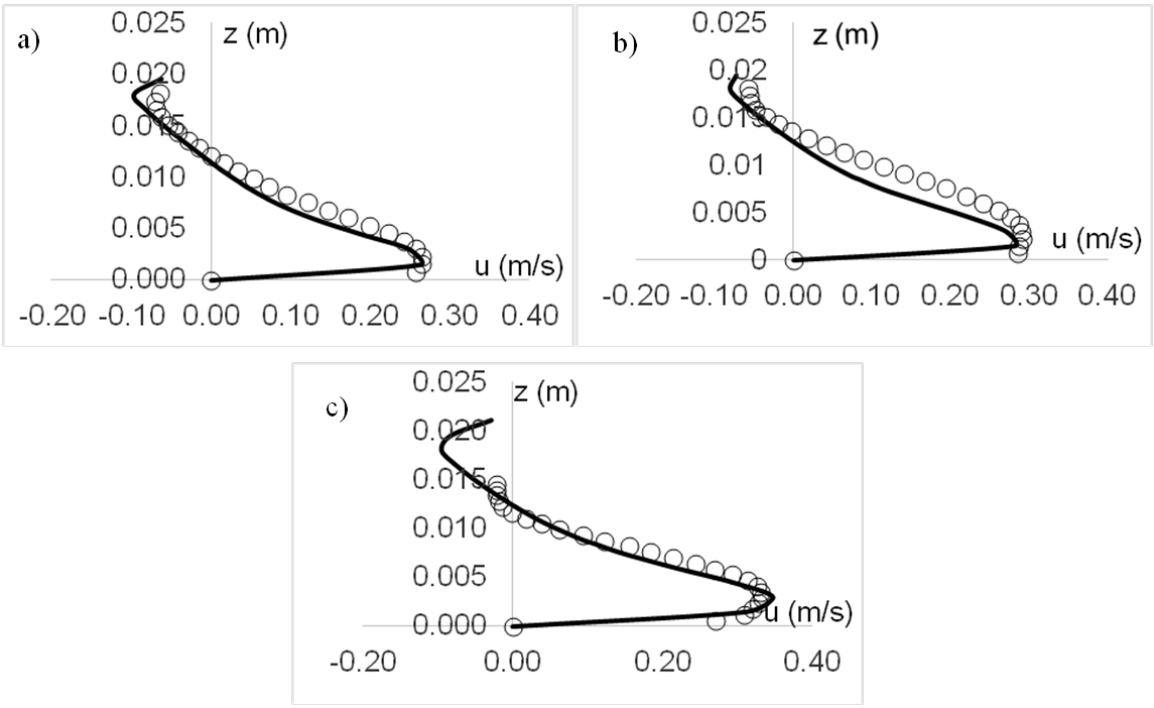

Figure 5. Experimental (open dots) and numerical (continuous line) profiles of local liquid velocity along the vertical line passing through the center of the recirculation area establishing inside each cavity for the flow rates per unit width (a) 1.11 10^{-3} $m^3s^{-1}m^{-1}$, (b) 1.48 10^{-3} $m^3s^{-1}m^{-1}$ and (c) 1.85 10^{-3} $m^3s^{-1}m^{-1}$.

The comparison between the values of the light flash-related hydrodynamic parameters predicted by the CFD and those computed from the post-processed experimental data is reported in Table 1.

Table 1. Comparison of experimentally determined and numerically simulated hydraulic features of potential photobiologic significance for the 6° channel slope.

Flow rate per unit width (m^3 s^{-1} m^{-1})	Recirculation period (s)		Transport stream flow transit time (s)		Recirculation area (10^{-4} m^2)		Total cross-section (10^{-4} m^2)		Ratio of recirculating area to total cross-section	
	Exp	Num	Exp	Num	Exp	Num	Exp	Num	Exp	Num
1.11 10^{-3}	0.37	0.34	0.31	0.31	3.83	4.43	8.58	9.27	0.45	0.48
1.48 10^{-3}	0.34	0.33	0.27	0.26	2.91	4.32	9.12	9.45	0.32	0.43
1.85 10^{-3}	0.27	0.29	0.25	0.23	2.14	3.97	9.23	9.87	0.23	0.40

Preprints (www.preprints.org) | NOT PEER-REVIEWED | Posted: 5 June 2019 doi:10.20944/preprints201906.0043.v1

It can be seen that the two period-related features are extremely consistent between corresponding flow rates, as deviations are within 10%. Larger deviations can be observed for the ratio of recirculating to total cross-section to which each feature applies only for the higher specific flow rates. This deviation is motivated by the increasingly agitated free surface which did not undergo the image analysis procedure. The discrepancy in the total cross-section of the liquid body contained by the cavity between CFD and experimental determination is constant across specific flow rates and is largely justified by the agitated free surface effect as well.

The CFD model was validated by attempting to predict the flow conditions that would establish if a wavy channel with the same geometry was installed at a higher installation angle, i.e., 9°. The simulations relevant to the channel inclined by 9° are characterized by the presence of a less stable free surface with respect to that obtained in the 6° inclination cases. Furthermore, the recirculation zones, although they are present, fluctuate over time never settling in a well-defined zone (not even when the simulation has reached the steady state).

Companion experimental tests were therefore performed with the channel slope set at 9° to assess the validity of CFD predictions. Post-processed experimental data did not show recirculations at larger specific flow rates (Q_2=0.8 m^3/h and Q_3=1.0 m^3/h, corresponding to 1.48 10^{-3} $m^3s^{-1}m^{-1}$ and 1.85 10^{-3} $m^3s^{-1}m^{-1}$ specific flow rates), while a small recirculation area was visible at the lower specific test flow rate (Q_1=0.6 m^3/h, corresponding to 1.11 10^{-3} m^3 s^{-1} m^{-1}). A deeper analysis carried out by visualizing the experimental tracer particles trajectories showed, however, that recirculation sections still appear at higher specific flow rates, but the positions of the centers of such recirculation sections fluctuate, so that they do not appear in streamline plots as a consequence of the averaging of velocity fields over the whole acquisition time of the experimental run. A constant finding of this closer observation is that the observed moving-center recirculation zones always lie above the transport stream. These findings appear very consistent and show that the developed CFD model is very robust and reliable.

Preprints (www.preprints.org) | NOT PEER-REVIEWED | Posted: 5 June 2019 doi:10.20944/preprints201906.0043.v1

Even in the absence of significant recirculation areas within the cavity, the transport stream produces an alternance of light and darkness, and the validated model at 9° slope was therefore used to attempt calculating the characteristic period (transport stream flow transit time) and the cross-sections which have a photobiological significance (Table 2). As a matter of facts, the 6°-to-9° increase in channel slope did not produce a significant decrease of the recirculation period.

The lowest recirculatory period of the tested installation slopes is 0.27 s (for both 6° and 9° slope), and the lowest top-bottom straight-transit time is 0.18 s (9° slope), corresponding to flashing frequencies of 3.7 Hz and 5.6 Hz, respectively. The validated CFD model might be reliably used to improve that result by optimizing relevant aspects of the geometry (pitch and inclination) and operation (specific flow rate) of the sloping wavy photobioreactor, hunting for an optimal synergism of the entailed flashing-light effects and mass transfer efficiency, and thereby improving microalgal productivity.

Table 2. Hydraulic features of potential photobiologic significance for validated model at 9° slope.

Flow rate per unit width ($m^3\ s^{-1}\ m^{-1}$)	Recirculation period (s)	Transport stream flow transit time (s)	Recirculation area ($10^{-4}\ m^2$)	Total cross-section ($10^{-4}\ m^2$)	Ratio of recirculating to total cross-section
$1.11\ 10^{-3}$	0.28	0.25	3.36	6.79	0.49
$1.48\ 10^{-3}$	0.29	0.23	3.31	7.84	0.42
$1.85\ 10^{-3}$	0.27	0.18	2.39	8.18	0.33

4 Conclusions

The present work shows that CFD modelling is capable to accurately predict hydrodynamic parameters which are relevant for photobiology, such as the recirculating and transport stream flow periods (within 10%) of stable flows. The developed model robustness was demonstrated by the successful prediction of the flow behaviour at a higher installation inclination of the wavy channel, where unstable recirculations clearly visible in the CFD streamlines match unstable recirculations which can be spotted by inspecting the experimental trajectories. The lowest recirculatory period of the tested installation slopes is 0.27 s,

and the lowest top-bottom straight-transit time is 0.18 s, corresponding to flashing frequencies of 3.7 Hz and 5.6 Hz, respectively.

The reliability of the presented CFD model paves the way to multiple development scenarios for the research to come, among which: (1) the improvement of flashing light frequency-related aspects of the geometry (pitch and inclination) and operation (specific flow rate) of the sloping wavy photobioreactor, (2) the development of a coupled fluid dynamic-cell photobiology model for the forecast of microalgal productivity of the bare photobioreactor, and (3) the experimental validation of the photobioreactor including the recirculation device with a living culture in controlled high irradiance experimental conditions and real-life outdoor operation.

Author Contributions

Conceptualization, Agnese Cicci; Investigation, Monica Moroni and Simona Lorino; Supervision, Marco Bravi.

Conflicts of Interest

The authors declare no conflict of interest.

References

[1] Kim, Z.H., Kim, S.H., Lee, H.S., Lee, C.G., 2006. Enhanced production of astaxanthin by flashing light using Haematococcus pluvialis. Enzyme Microb. Technol. 39, 414–419.

[2] Pruvost, J., Le Borgne, F., Artu, A., Cornet, J.F. and Legrand, J., 2016. Industrial photobioreactors and scale-up concepts. In Advances in Chemical Engineering (Vol. 48, pp. 257-310). Academic Press.

[3] Raven, J.A., 2011. The cost of photoinhibition. Physiol. Plant. 142, 87–104.

[4] Grobbelaar, J.U., 2009. Upper limits of photosynthetic productivity and problems of scaling. J Appl. Phycol. 21, 519-522.

 doi:10.20944/preprints201906.0043.v1

[5] Vejrazka, C., Janssen, M., Streefland, M., & Wijffels, R. H. (2012). Photosynthetic efficiency of Chlamydomonas reinhardtii in attenuated, flashing light. Biotechnology and bioengineering, 109(10), 2567-2574.

[6] Xue, S., Zhang, Q., Wu, X., Yan, C. and Cong, W., 2013. A novel photobioreactor structure using optical fibers as inner light source to fulfill flashing light effects of microalgae. Bioresource technology, 138, pp.141-147.

[7] Graham, P.J., Nguyen, B., Burdyny, T. and Sinton, D., 2017. A penalty on photosynthetic growth in fluctuating light. Scientific reports, 7, 1-11.

[8] Grobbelaar, J.U., 2006. Photosynthetic response and acclimation of microalgae to light fluctuations. In: Algal cultures, analogues of blooms and applications (ed. D.V. Subba Rao). Science Publishers, Enfield (USA), 671-683.

[10] Richmond, A., 1996. Efficient utilization of high irradiance for production of photoautotropic cell mass: a survey. Journal of Applied Phycology, 8(4-5), pp.381-387.

[11] Abu-Ghosh, S., Fixler, D., Dubinsky, Z, Iluz, D., 2016. Flashing light in microalgae biotechnology. Bioresource Technology 203, 357-363.

[12] Gordon, J.M., Polle, J.E., 2007. Ultrahigh bioproductivity from algae. Applied Microbiology and Biotechnolog. 76(5), 969-975.

[13] Qiang, H., Richmond, A., 1996. Productivity and photosynthetic efficiency of Spirulina platensis as affected by light intensity, algal density and rate of mixing in a flat plate photobioreactor. Journal of Applied Phycology, 8 (2), 139-145.

[14] Grobbelaar, J.U., 1994. Turbulence in mass algal cultures and the role of light/dark fluctuations. J. Appl. Phycol. 6, 331-335.

[15] Scarsella, M., Torzillo, G., Cicci, A., Belotti, G., De Filippis, P., Bravi, M., 2011. Mechanical stress tolerance of two microalgae. Process biochem. 47(11), 1603-1611.

[16] Cicci, A., Stoller, M., Moroni, M., Bravi, M., 2015. Mass Transfer, Light Pulsing and Hydrodynamic Stress Effects in Photobioreactor Development. Chem. Eng. Transaction 43, 235-240.

[17] Torzillo, G., Giannelli, L., Verdone, N., De Filippis, P., Scarsella, M., Martínez-Roldán, A.J., Bravi, M., 2010. Microalgae Culturing in Thin-layer Photobioreactors. Chem. Eng. Transaction 20, 265-270.

[18] Setlik, I., Veladimir, S., Malek, I., 1970. Dual purpose open circulation units for large scale culture of algae in temperature zones. Basic design considerations scheme of pilot plant. Algol Stud (Trebon). 1-11.

[19] Moroni, M., Cicci, A., Bravi, M., 2014. Experimental investigation of a local recirculation photobioreactor for mass cultures of photosynthetic microorganisms. Water Research 52, 29-39.

[20] Sforza, E., Simionato, D., Giacometti, G.M., Bertucco, A., Morosinotto, T., 2012. Adjusted light and dark cycles can optimize photosynthetic efficiency in algae growing in photobioreactors. PloS one 7(6), e38975.

[21] Soman, A. and Shastri, Y., 2015. Optimization of novel photobioreactor design using computational fluid dynamics. Applied energy, 140, pp.246-255.

[22] Gómez-Pérez, C.A., Espinosa, J., Ruiz, L.M. and Van Boxtel, A.J.B., 2015. CFD simulation for reduced energy costs in tubular photobioreactors using wall turbulence promoters. Algal research, 12, pp.1-9.

[23] Cho, Bovinille Anye, and Robert William McClelland Pott. "The development of a thermosiphon photobioreactor and analysis using Computational Fluid Dynamics (CFD)." Chemical Engineering Journal 363 (2019): 141-154.

[24] Hirt, C.W., Nichols, B.D., 1981. Volume of Fluid (VOF) Method for Dynamics of Free Boundaries. J. Comput. Phys. 39, 201.

 doi:10.20944/preprints201906.0043.v1

[25] Moroni, M., Lupo, E., La Marca, F., 2017. Investigation on an innovative technology for wet separation of plastic wastes. Waste Management 66, 13-22.